forests

MDPI

Article

Effects of *Myo*-Inositol on NaCl Stress in *Tamarix ramosissima*: Insights from Transcriptomics and Metabolomics

Haijia Li [1,2,†], Yunlong Fan [3], Huanchao Zhang [1,*] and Yahui Chen [1,2,*,†]

[1] Collaborative Innovation Center of Sustainable Forestry in Southern China of Jiangsu Province, Nanjing Forestry University, Nanjing 210037, China; haijiali@njfu.edu.cn
[2] Jiangsu Academy of Forestry, Nanjing 211153, China
[3] Department of Statistics, Faculty of Science, University of British Columbia, Vancouver, BC V6T 1Z4, Canada; mo0514@student.ubc.ca
* Correspondence: hczhang@njfu.edu.cn (H.Z.); chenyahui@njfu.edu.cn (Y.C.)
† These authors contributed equally to this work.

Abstract: NaCl stress adversely affects plant growth. *Tamarix ramosissima* Ledeb (*T. ramosissima*), a halophyte, thrives in saline-alkali areas. *Myo*-inositol, a lipid-soluble compound, is crucial for stress response, but its role in mitigating NaCl damage remains underexplored. We analyzed transcriptome sequencing and metabolites in *T. ramosissima* roots under NaCl stress at various intervals (0 h, 48 h, and 168 h). We identified ten *Myo*-inositol oxygenase-related genes. Nine of these genes, linked to metabolic pathways involving *Myo*-inositol, showed differential expression. *Myo*-inositol accumulation increased over time, suggesting its role as an osmotic regulator and reactive oxygen species (ROS) scavenger. This accumulation likely shields *T. ramosissima* from NaCl-induced osmotic and oxidative damage. Notably, *Unigene0002140* and *Unigene0095980*, associated with *Myo*-inositol oxygenase, appear to regulate *Myo*-inositol accumulation and correlate significantly with its levels. We hypothesize they are key genes in controlling *Myo*-inositol levels, warranting further study. This research illuminates the role of *Myo*-inositol oxygenase-related genes in *T. ramosissima* roots combating NaCl stress, offering insights for selecting salt-tolerant tree species.

Keywords: *Myo*-inositol; metabolite; NaCl stress; *Tamarix ramosissima*; transcriptome

Citation: Li, H.; Fan, Y.; Zhang, H.; Chen, Y. Effects of *Myo*-Inositol on NaCl Stress in *Tamarix ramosissima*: Insights from Transcriptomics and Metabolomics. *Forests* **2023**, *14*, 1686. https://doi.org/10.3390/f14081686

Academic Editor: Richard S. Dodd

Received: 18 July 2023
Revised: 12 August 2023
Accepted: 17 August 2023
Published: 21 August 2023

1. Introduction

In recent years, the saline soil area has expanded due to climate change and human activities. More than 3% of the world's soil resources are affected by salinity [1]. It is estimated that by 2050, more than 50% of the world's arable land will be affected by salinization [2,3], posing a serious environmental problem that threatens the development of sustainable agriculture, forestry, and future food security. Therefore, the efficient utilization of saline soil has become an urgent issue to be resolved [4]. Importantly, NaCl is one of the most widely distributed salts in saline soils, and it can have negative effects on various physiological and biochemical processes at different stages of plant growth and development, ultimately leading to NaCl stress [5,6].

NaCl stress is one of the most significant types of abiotic stress, posing a severe threat to the development of agriculture and forestry [7,8]. NaCl stress is a complex mechanism that affects almost all growth physiological pathways during plant growth and development [9,10]. NaCl stress can cause membrane disintegration, toxic metabolite production, inhibition of photosynthesis, generation of reactive oxygen species (ROS), and weakened nutrient acquisition capacity in plants, leading to cell and whole plant death [11–14]. Therefore, NaCl stress is a major factor limiting plant growth [15]. Notably, the plant organ that first senses stress signals under NaCl stress is the root, which is also the most directly damaged [16–18]. Under normal growth conditions, plant roots can absorb water and nutrients to maintain cellular homeostasis [19]. Still, NaCl stress inhibits root respiration and disrupts root

metabolism, leading to internal root dysfunction, ultimately destroying this balance and affecting plant growth [20]. Inositol, a type of cyclohexanehexol, is a prevalent small molecule found throughout the biological realm. It boasts a notably stable structural and chemical profile. Of its nine isomers, *Myo*-inositol stands out as the most biologically active [21,22]. *Myo*-inositol is a class of small molecule compounds that are essential for life growth and development [23,24]. It also acts as the structural cornerstone for various lipid signaling molecules that modulate complex cellular pathways, encompassing stress responses and the production of ascorbic acid [25]. Notably, inositol signaling is postulated to be pivotal in diverse facets of plant development and resilience [26]. *Myo*-inositol and its derivative metabolites are widely present in all eukaryotes. They play significant roles in stress responses and developmental processes, functioning as both lipids and soluble compounds [24,26,27]. Inositol phosphatases, vital in the synthesis and breakdown of *Myo*-inositol and its derivatives, can remove the phosphate from the inositol ring, influencing inositol signaling [26]. Studies by Eisenberg and Kindl [28] have shown that the synthesis pathway of inositol includes the following steps: D-Glucose is phosphorylated to generate D-Glucose-6-phosphate by hexokinase (HK). D-Glucose-6-phosphate is then cyclized to form *Myo*-inositol-1-phosphate by *Myo*-inositol-1-phosphate synthase (MIPS). *Myo*-inositol-1-phosphate is subsequently dephosphorylated by inositol monophosphatase (IMP) to produce inositol finally. Particularly, the cyclization process of D-Glucose-6-phosphate is irreversible, and MIPS plays a crucial role in this step [29]. Furthermore, inositol acts as a compatible solute to balance cell expansion and can enhance various basic metabolisms to adapt to NaCl stress [30]. Moreover, it serves as an osmoprotectant and ROS scavenger to protect plants from osmotic stress and oxidative damage. It also functions as a signaling molecule, regulating many plant metabolic pathways and enhancing salt tolerance [31]. Hu et al. noted that external *Myo*-inositol under NaCl stress increases sugar levels, enhances antioxidant activity, reduces Na^+ absorption, and removes ROS in Malus hupehensis Rehd [32].

Tamarix ramosissima Ledeb (*T. ramosissima*) is a salt-excreting halophyte that has developed efficient abiotic stress tolerance systems to adapt to adverse environments and cope with abiotic stress [33], such as root salt avoidance and salt gland secretion [34,35]. However, research indicates that *T. ramosissima* normally grows under NaCl concentrations below 100 mM, while concentrations above 200 mM affect its regular growth [36]. Consequently, this study integrates transcriptomics and metabolomics to delve into the role of *Myo*-inositol in the roots of *T. ramosissima* under NaCl stress at a molecular level. Our objective is to pinpoint key genes and metabolic pathways. This research will lay a scientific and theoretical foundation and provide genetic resources for the exploration of NaCl stress resistance and enhancement of salt tolerance in *Tamarix* plants.

2. Materials and Methods

2.1. Experimental Materials and NaCl Treatment

For this experiment, cuttings of *T. ramosissima* with similar growth and five-month age were selected and cultured in hydroponic boxes (twenty-four holes) with 1/2 Hoagland's nutrient solution. The nutrient solution was replaced every three days (cultivation environment: temperature 26 ± 2 °C, relative humidity: 40%~55%). After two months, the plants were ready for use. Every experiment had a control and a treatment group, with eight plants in each. This was repeated three times. Plants cultured in 1/2 Hoagland's nutrient solution served as the control group, while those cultured in 1/2 Hoagland's nutrient solution supplemented with 200 mM NaCl formed the treatment group. The nutrient solution was replaced every three days. Root samples were collected at 0 h, 48 h, and 168 h after treatment and were used for transcriptome sequencing and metabolite detection.

2.2. Transcriptome Sequencing and Differentially Expressed Genes Screening

We selected root samples from treated *T. ramosissima* and sent them to biotechnology company. (GENE Denovo, Guangzhou, China) for transcriptome sequencing.

RNA was isolated using the Invitrogen kit (Beinuo Bio, Shanghai, China). Following isolation, mRNA was enriched with oligo (dT) cellulose and then segmented to an average length of 200 nt with a fragmentation buffer from New England Biolabs (#E7530). Utilizing random hexamer primers, the first-strand cDNA synthesis occurred, succeeded by the creation of the second-strand cDNA using DNA polymerase I and RNase H. Subsequent steps included the purification of the cDNA fragments, the addition of a terminal "A" base, and their ligation to Illumina adapters. Size selection was conducted on an agarose gel, from which appropriate fragments were isolated and subjected to PCR amplification. The sequenced reads of these fragments were generated on the Illumina HiSeq system by biotechnology company Company (GENE Denovo, Guangzhou, China) [37].

The raw data obtained from transcriptome sequencing was submitted to the Short Reads Archive (SRA) database of the National Center for Biotechnology Information (NCBI) with an SRP number of SRP356215. We conducted DEG screening on the obtained data [38] and annotated them to the Gene Ontology (GO) [39] and Kyoto Encyclopedia of Genes and Genomes (KEGG) [40] for enrichment analysis.

2.3. Metabolite Extraction, Detection and Differential Metabolite Screening

T. ramosissima root samples, after treatment, were submitted to a biotechnology company (GENE Denovo, Guangzhou, China) for metabolites extraction and metabolites detection, then analyzed via liquid chromatography–mass spectrometry (LC–MS). The LC–MS analysis employed a Vanquish UHPLC system from Thermo Fisher, Bremen, Germany, which was integrated with an Orbitrap Q Exactive^{TM} HF-X mass spectrometer. These samples were channeled into a Hypersil Gold column measuring 100 × 2.1 mm with a 1.9 µm particle size, applying a linear gradient over 17 min at a flow rate of 0.2 mL/min.

For positive polarity mode, the eluents used were eluent A, which is 0.1% FA in water, and eluent B, methanol. Conversely, in the negative polarity mode, we utilized eluent A, which is 5 mM ammonium acetate at pH 9.0, and eluent B, methanol. We followed a solvent gradient pattern: starting with 2% B for 1.5 min, ramping up to 100% B over 12 min, holding at 100% B for 14 min, dropping to 2% B by the 14.1-min mark, and then maintaining 2% B for the remainder up to 17 min.

The Q Exactive^{TM} HF-X spectrometer operated in both positive and negative modes, set with a 3.2 kV spray voltage, a capillary temperature at 320 °C, and gas flows of 40 arb for sheath and 10 arb for auxiliary [41]. We performed differential metabolite screening and *p*-value testing on the acquired data and annotated the obtained differential metabolites to the KEGG database (www.kegg.jp/kegg/pathway.html accessed on 16 June 2023) [42].

2.4. Quantitative Real-Time PCR Validation of Candidate Genes

We randomly selected ten candidate genes to verify the accuracy of the transcriptome sequencing results. We used the RNAprep pure kit (Tiangeng, Beijing, China) to extract total RNA from the root samples of *T. ramosissima* and synthesized cDNA using the Prime Script^{TM}DEG II1st Strandc DNA Synthesis Kit (Takara, Beijing, China). Primers were designed using Primer Premier 5 software (Supplementary Table S1). The samples were analyzed using the SYBR Green Realtime PCR Master Mix (TOYBO, Jinan China) on the ABI ViiA™ 7 Real-time PCR system (ABI, California, CA, USA). Each gene was biologically replicated three times, using Tubulin as an internal reference gene. The relative expression levels were calculated using the $2^{-\Delta\Delta Ct}$ method [43].

2.5. Prediction of Pfam Protein Structure Domains

We compared the protein sequences of the candidate genes in the Pfam database [44] to obtain annotations of the structural domains.

2.6. Experiment Processing

We used Microsoft Excel (Microsoft, Washington, DC, USA) to perform data calculation and processing. This included calculating the mean, standard deviation of the raw data,

and $\log_2$ fold change. SPSS 26.0 software (SPSS, New York, NY, USA) was used for ANOVA analysis with LSD post-hoc test. Finally, the data were plotted using Origin 2018 software (OriginLab Corporation, Northampton, MA, USA).

3. Results

3.1. Analysis of Myo-Inositol in the Roots of T. ramosissima under NaCl Stress

The metabolites in the roots of *T. ramosissima* were detected and analyzed by LC–MS under NaCl stress at 0 h, 48 h, and 168 h. The results indicated that Myo-inositol was annotated to eight KEGG pathways (Table 1): metabolic pathways (ko01100), microbial metabolism in diverse environments (ko01120), biosynthesis of antibiotics (ko01130), ABC transporters (ko02010), Galactose metabolism (ko00052), ascorbate and aldarate metabolism (ko00053), Inositol phosphate metabolism (ko00562), phosphatidylinositol signaling system (ko04070). The *Myo*-inositol content (Log_2 fold-change) exhibited a slight decrease under NaCl stress at 48 h. However, with the increase of NaCl stress time, the *Myo*-inositol content (Log_2 fold-change) demonstrated a significant increase trend under NaCl stress at 168 h (Figure 1).

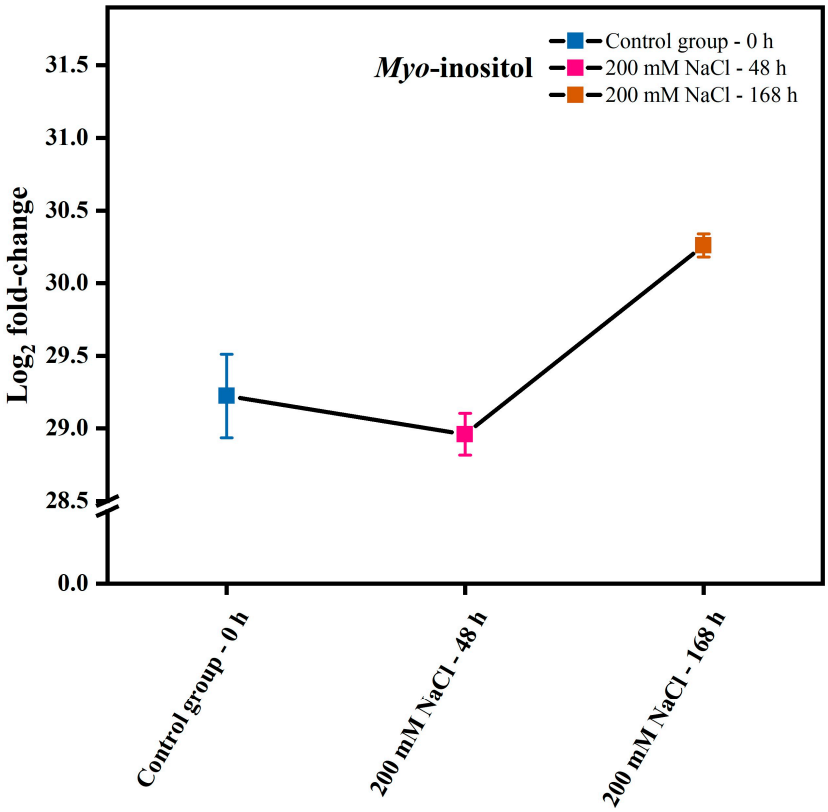

Figure 1. Trend graph of Log_2 fold-change of *Myo*-inositol content. (The trend of Log_2 fold-change in *Myo*-inositol content in the roots of *T. ramosissima* under NaCl stress at 48 h and 168 h).

Table 1. Information on *Myo*-inositol.

Name	Formula	Molecular Weight	PPM	RT (min)	m/z	Pathway
Myo-inositol	$C_6H_{12}O_6$	180.06	2.43	1.26	181.07	ko01100; ko01120; ko01130; ko02010; ko00052; ko00053; ko00562; ko04070

Note: ko01100 is Metabolic pathways; ko01120 is Microbial metabolism in diverse environments; ko01130 is Biosynthesis of antibiotics; ko02010:ABC transporters; ko00052: Galactose metabolism; ko00053: ascorbate and aldarate metabolism; ko00562: Inositol phosphate metabolism; ko04070: Phosphatidylinositol signaling system.

3.2. Analysis of Myo-Inositol Oxygenase-Related Genes in the Roots of T. ramosissima under NaCl Stress

Based on the roots of *T. ramosissima* under NaCl stress at 48 h and 168 h, we identified ten *Myo*-inositol oxygenase-related genes (Table 2). With the exception of *Unigene0006165*, which was not annotated to any KEGG pathway, the remaining nine genes were all linked to three KEGG pathways: metabolic pathways (ko01100), ascorbate and aldarate metabolism (ko00053), and Inositol phosphate metabolism (ko00562). Moreover, judging by their expression levels (Supplementary Figure S1), three genes (*Unigene0002140*, *Unigene0032727*, and *Unigene0056095*) initially demonstrated a decrease in expression, which was later followed by an increase under NaCl stress at the checkpoint of the 48 h and 168 h marks. There were five genes (*Unigene0006163*, *Unigene0006164*, *Unigene0006165*, *Unigene0032727*, and *Unigene0067118*) whose expression levels first increased and then decreased at 48 h and 168 h under NaCl stress. Significantly, these genes were considerably upregulated at 48 h under NaCl stress compared to the control group. It's also worth noting that *Unigene0095980* did not exhibit any change in expression levels under NaCl stress at both 0 h and 48 h but was markedly upregulated at 168 h.

Table 2. Analysis of *Myo*-inositol oxygenase-related genes.

ID	Description	Log_2 Fold-Change			Pathway
		CK-0 h vs. N-48 h	N-48 h vs. N-168 h	CK-0 h vs. N-168 h	
Unigene0002140	*Myo*-inositol oxygenase	−3.61	4.95	1.34	ko01100; ko00053; ko00562
Unigene0095980	*Myo*-inositol oxygenase-like	0.00	9.36	9.36	ko01100; ko00053; ko00562
Unigene0032727	*Myo*-inositol oxygenase 1-like	−2.36	1.68	−0.68	ko01100; ko00053; ko00562
Unigene0095469	*Myo*-inositol oxygenase-like	12.33	−12.33	0.00	ko01100; ko00053; ko00562
Unigene0006164	*Myo*-inositol oxygenase	11.13	−11.13	0.00	ko01100; ko00053; ko00562
Unigene0006165	Predicted: *Myo*-inositol oxygenase 1-like isoform X2	11.52	−11.52	0.00	-
Unigene0017638	*Myo*-inositol oxygenase-like	−6.59	0.00	−6.59	ko01100; ko00053; ko00562
Unigene0056095	*Myo*-inositol oxygenase 1-like	−1.41	0.36	−1.06	ko01100; ko00053; ko00562
Unigene0006163	*Myo*-inositol oxygenase-like	10.04	−10.04	0.00	ko01100; ko00053; ko00562
Unigene0067118	*Myo*-inositol oxygenase 1-like	7.06	−7.06	0.00	ko01100; ko00053; ko00562

Note: control group-0 h:CK-0 h; 200 mM NaCl-48 h: N-48 h; 200 mM NaCl-168 h: N-168 h; ko01100: Metabolic pathways; ko00053: ascorbate and aldarate metabolism pathway; ko00562: Inositol phosphate metabolism pathway.

3.3. Pfam A Protein Structure Domain Analysis of Myo-Inositol Oxygenase-Related Genes in the Roots of T. ramosissima

We aligned the protein sequences of the ten Myo-inositol oxygenase-related genes, identified in the roots of *T. ramosissima* under NaCl stress, to the PfamA database and analyzed them (Supplementary Table S2). The results revealed that the predicted structural domains of the Unigene-encoded protein sequences by the HMM model of *Myo*-inositol oxygenase-related genes are from position 1 to 319. The HMM length al 249, the bit score ranging from 34.5 to 417.7, hmm acc as PF05153.15, clan as CL0237, and PfamA_definition as *Myo-inositol* oxygenase.

3.4. Analysis of the Ascorbate and Aldarate Metabolism Pathway in the Roots of T. ramosissima under NaCl Stress

Based on the analysis of the ascorbate and aldarate metabolism pathway (Table 3), in the control group-0 h vs. 200 mM NaCl-48 h (CK-0 h vs. N-48 h) comparison group, there are thirty-one differentially expressed genes (DEGs) and one differentially annotated metabolite in the ascorbate and aldarate metabolism pathway. Within them, nineteen DEGs were upregulated, and twelve DEGs were downregulated. In the 200 mM NaCl-48 h vs. 200 mM NaCl-168 h (Na-48 h vs. N-168 h) comparison group, there were thirty-four DEGs and two differentially annotated metabolites in the ascorbate and aldarate metabolism pathway. Among them, thirteen DEGs were upregulated, and twenty-one DEGs were downregulated. In the control group-0 h vs. 200 mM NaCl-168 h (CK-0 h vs. N-168 h) comparison group, there were sixteen DEGs and four differentially annotated metabolites in the ascorbate and aldarate metabolism pathway, and the differentially annotated metabolites in ascorbate and aldarate metabolism showed significant differences ($p < 0.05$). Amid them, there were eight upregulated and eight downregulated DEGs.

Table 3. Analysis of ascorbate and aldarate metabolism pathway in the roots of *T. ramosissima* under NaCl stress.

Pathway	Annotated Genes	Up	Down	Gene_*p*-Value	Annotated Metabolites	Metabolite_*p*-Value	Pathway ID
				CK-0 h vs. N-48 h			
Ascorbate and aldarate metabolism	31	19	12	0.713618	1	0.735061	ko00053
				N-48 h vs. N-168 h			
Ascorbate and aldarate metabolism	34	13	21	0.645249	2	0.276678	ko00053
				CK-0 h vs. N-168 h			
Ascorbate and aldarate metabolism	16	8	8	0.849475	4	0.033218	ko00053

Note: control group-0 h:CK-0 h; 200 mM NaCl-48 h: N-48 h; 200 mM NaCl-168 h: N-168 h.

3.4.1. Analysis of Differentially Expressed Genes in Ascorbate and Aldarate Metabolism Pathway

Based on the roots of *T. ramosissima* under NaCl stress at 48 h and 168 h, we analyzed the forty-three DEGs annotated in the ascorbate and aldarate metabolism pathway (Supplementary Table S3). We found that in the CK-0 h vs. N-48 h, CK-0 h vs. N-168 h, and Na-48 h vs. N-168 h comparison groups, there are two common DEGs (*Unigene0015725* and *Unigene0011551*). The results of Supplementary Figure S2 show that in the root of *T. ramosissima* under NaCl stress at 48 h and 168 h, the expression levels of eight DEGs (*Unigene0066846*, *Unigene0037768*, *Unigene0105617*, *Unigene0002140*, *Unigene0032727*, *Unigene0105238*, *Unigene0102888*, and *Unigene0064911*) first decreased and then increased.

Notably, the expression levels of seven DEGs (*Unigene0056095*, *Unigene0105480*, *Unigene0021103*, *Unigene0021104*, *Unigene0017008*, *Unigene0095536*, and *Unigene0105664*) consistently increased. In addition, *Unigene0095980* showed no change in expression levels under NaCl stress at 0 h and 48 h, but its expression level was significantly increased under NaCl stress at 168 h.

3.4.2. Analysis of Differential Metabolites in the Ascorbate and Aldarate Metabolism Pathway

From studying the *T. ramosissima* roots subjected to NaCl stress for 48 and 168 h, we identified a total of four differential metabolites linked to the ascorbate and aldarate metabolism pathway (Figure 2). In the comparison group of CK-0 h vs. N-48 h, one differential metabolite (L-Threonate) was annotated, and it was degraded. In the comparison group of N-48 h vs. N-168 h, two differential metabolites (*Myo*-inositol and L-Gulono-1,4-lactone) were annotated, and both were accumulating. In the comparison group of CK-0 h vs. N-168 h, four differential metabolites (*Myo*-inositol, 4-lactone, L-Gulono-1, L-Threonate, and 2-Oxoglutarate) were annotated. Among them, *Myo*-inositol and L-Gulono-1,4-lactone were accumulating, while L-Threonate and 2-Oxoglutarate were degrading (Supplementary Table S4). The results show that in the roots of *T. ramosissima* under NaCl stress for 48 h and 168 h, the content of *Myo*-inositol, 4-lactone, L-Gulono-1, and L-Threonate first decreased and then increased. The content of *Myo*-inositol and L-Gulono-1,4-lactone under NaCl stress 168 h was significantly different from the control group (Supplementary Figure S3). The content of 2-Oxoglutarate showed a decreasing trend under NaCl stress for 48 h and 168 h, and its content in NaCl stress for 48 h and 168 h was significantly different from the control group.

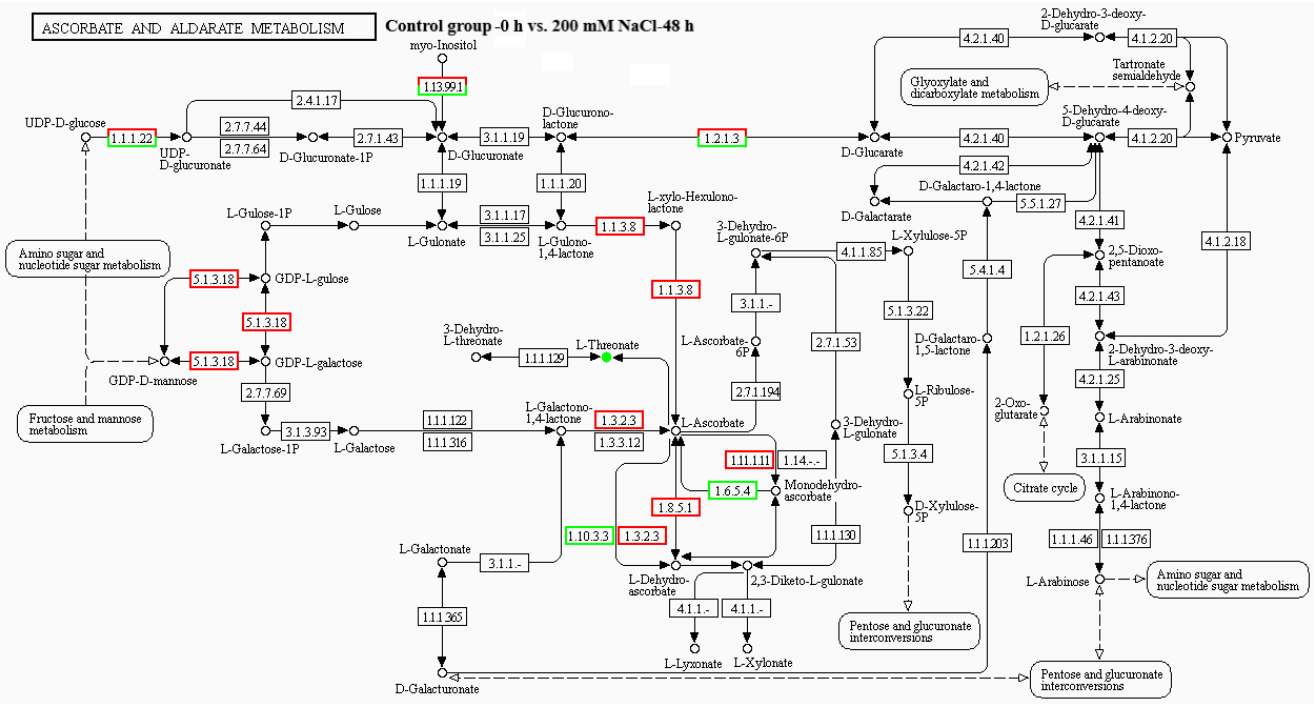

Figure 2. *Cont.*

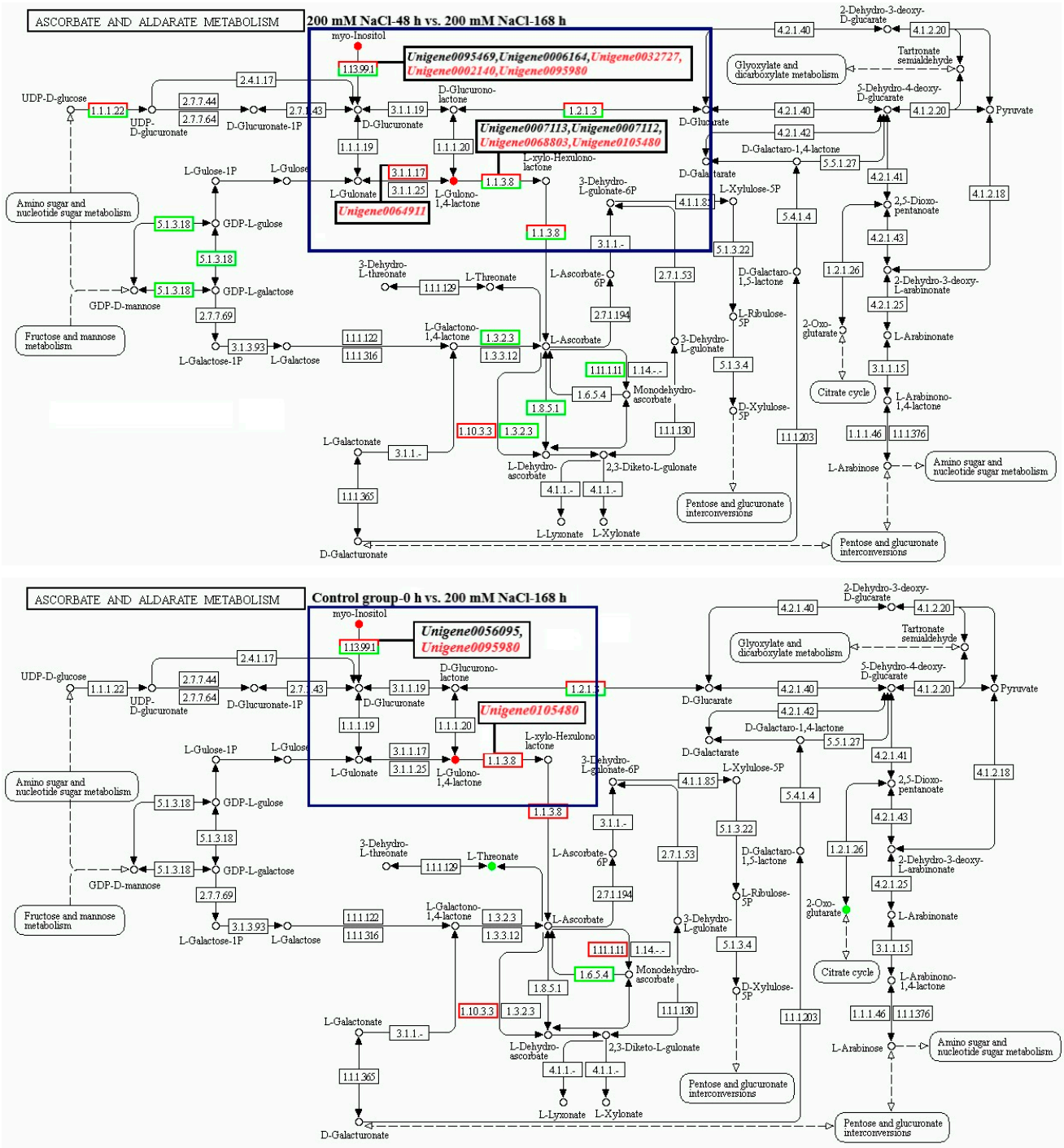

Figure 2. Analysis of the ascorbate and aldarate metabolism pathway. (*T. ramosissima* root annotated DEGs and differential metabolites in the ascorbate and aldarate metabolism pathway under NaCl stress at 0 h, 48 h, and 168 h. Note: blue box: DEGs annotated to metabolic pathways regulate the metabolism of different metabolites; ●: accumulation of differential metabolites; ●: degradation of differential metabolites; black genes in the box: decrease in the expression levels of DEGs; red genes in the box: increase in the expression levels of differentially expressed genes).

3.4.3. Pearson Correlation Analysis of Differentially Expressed Genes and Their Related Differential Metabolites in the Ascorbate and Aldarate Metabolism Pathway

According to the absolute Pearson correlation coefficient $|\text{Corr}| > 0.8$ and $p < 0.05$ requirement, we performed Pearson correlation analysis on the DEGs and their related differential metabolites in the ascorbate and aldarate metabolism pathway (Figure 2).

The results show (Figure 3) that in the comparison group of 200 mM NaCl-48 h vs. 200 mM NaCl-168 h, there are five DEGs (*Unigene0095469*, *Unigene0006164*, *Unigene0032727*, *Unigene0002140*, and *Unigene0095980*) located downstream of *Myo*-inositol regulating the accumulation of *Myo*-inositol. Within them, *Unigene0095469* and *Unigene0006164* negatively regulate the accumulation of *Myo*-inositol, with no significant correlation. *Unigene0032727*, *Unigene0002140*, and *Unigene0095980* positively regulate the accumulation of *Myo*-inositol. Significantly, *Unigene0002140* and *Unigene0095980* positively regulate the accumulation of *Myo*-inositol and have a significant correlation. *Unigene0064911* is located upstream of L-Gulono-1,4-lactone, positively regulating the accumulation of L-Gulono-1,4-lactone, with a significant correlation. *Unigene0007112*, *Unigene0007113*, *Unigene0068803*, and *Unigene0105480* are located downstream of L-Gulono-1,4-lactone regulating the accumulation of L-Gulono-1,4-lactone. Among them, *Unigene0007112* and *Unigene0007113* negatively regulate the accumulation of L-Gulono-1,4-lactone, with *Unigene0007112* showing a significant correlation with L-Gulono-1,4-lactone. *Unigene0068803* and *Unigene0105480* positively regulate the accumulation of L-Gulono-1,4-lactone with no significant correlation. In the comparison group of CK-0 h vs. N-168 h, there are two DEGs (*Unigene0056095* and *Unigene0095980*) located downstream of *Myo*-inositol regulating the accumulation of *Myo*-inositol. Amid them, *Unigene0056095* negatively regulates the accumulation of *Myo*-inositol. In contrast, *Unigene0095980* positively regulates the accumulation of *Myo*-inositol and has a significant correlation. *Unigene0105480* is located downstream of L-Gulono-1,4-lactone, regulating the accumulation of L-Gulono-1,4-lactone with no significant correlation.

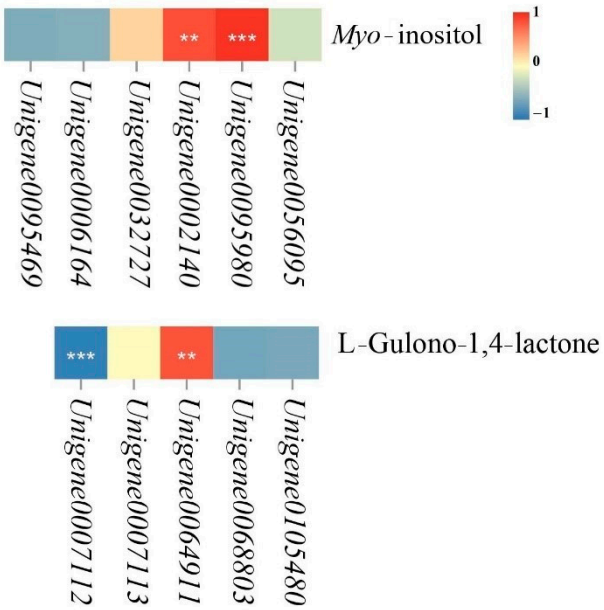

Figure 3. Pearson correlation analysis of DEGs and their related differential metabolites in the ascorbate and aldarate metabolism pathway. (*T. ramosissima* roots under NaCl stress at 48 h and 168 h annotated DEGs and their related differential metabolites in the ascorbate and aldarate metabolism pathway Pearson correlation analysis. Note: $p \geq 0.05$ is not marked; $0.001 < p < 0.01$ is marked as **; $p \leq 0.001$ is marked as ***).

3.5. Analysis of in Inositol Phosphate Metabolism Pathway in the Roots of T. ramosissima under NaCl Stress

Based on the analysis of the inositol phosphate metabolism pathway (Table 4), in the CK-0 h vs. N-48 h comparison group, there are thirty DEGs in the inositol phosphate metabolism pathway. Within them, eighteen DEGs were upregulated, and twelve DEGs were downregulated. However, no differentially expressed metabolites were annotated to the inositol phosphate metabolism pathway. In the N-48 h vs. N-168 h comparison group, there were twenty-seven DEGs and two differentially annotated metabolites in

the inositol phosphate metabolism pathway. Among them, nine DEGs were upregulated, and twelve DEGs were downregulated. In the CK-0 h vs. N-168 h comparison group, there were twelve DEGs and one differentially annotated metabolite in the inositol phosphate metabolism pathway. Amid them, there were four upregulated and wight downregulated DEGs.

Table 4. Analysis of inositol phosphate metabolism pathway in the roots of *T. ramosissima* under NaCl stress.

Pathway	Annotated Genes	Up	Down	Gene_*p*-Value	Annotated Metabolites	Metabolite_*p*-Value	Pathway ID
				CK-0 h vs. N-48 h			
Inositol phosphate metabolism	30	18	12	0.632468	0	-	ko00562
				Na-48 h vs. N-168 h			
Inositol phosphate metabolism	27	9	18	0.911003	2	0.066648	ko00562
				CK-0 h vs. N-168 h			
Inositol phosphate metabolism	12	4	8	0.965830	1	0.482970	ko00562

Note: control group-0 h:CK-0 h; 200 mM NaCl-48 h: N-48 h; 200 mM NaCl-168 h: N-168 h.

3.5.1. Analysis of Differentially Expressed Genes in the Inositol Phosphate Metabolism Pathway

There are thirty-six DEGs annotated to the Inositol phosphate metabolism pathway in the roots of *T. ramosissima* under NaCl stress (Supplementary Table S5). As shown in Supplementary Figure S4, the expression levels of eight DEGs (*Unigene0032727*, *Unigene0002140*, *Unigene0097496*, *Unigene0023711*, *Unigene0069542*, *Unigene0068974*, *Unigene0077925*, and *Unigene0037080*) first decreased and then increased. The expression levels of three DEGs (*Unigene0056095*, *Unigene0101311*, and *Unigene0105664*) have been consistently increasing. Notably, *Unigene0026986* and *Unigene0095980* did not change expression levels under NaCl stress at 0 h and 48 h, but their expression levels significantly increased under NaCl stress at 168 h.

3.5.2. Analysis of Differential Metabolites in the Inositol Phosphate Metabolism Pathway

There are two differentially expressed metabolites annotated to the Inositol phosphate metabolism pathway in the roots of *T. ramosissima* under NaCl stress (Supplementary Table S6). The results show (Figure 4) that no differentially expressed metabolites were annotated in the comparison group of CK-0 h vs. N-48 h. In the comparison group of Na-48 h vs. N-168 h, two differentially expressed metabolites were annotated (D-Glucose 6-phosphate and *Myo*-inositol). D-Glucose 6-phosphate is being degraded, while *Myo*-inositol is accumulating. At the same time, *Myo*-inositol content decreased at first and then increased at 48 h and 168 h under NaCl stress, and there is a significant difference in the concentration of *Myo*-inositol at 168 h of NaCl stress compared to the control group (Supplementary Figure S5). The concentration of D-Glucose 6-phosphate continues to decrease at 48 h and 168 h under NaCl stress, and there is a significant difference in its concentration at 168 h under NaCl stress compared to the control group (Supplementary Figure S5). In the comparison group of CK-0 h vs. N-168 h, one differentially expressed metabolite was annotated (*Myo*-inositol), and it is accumulating.

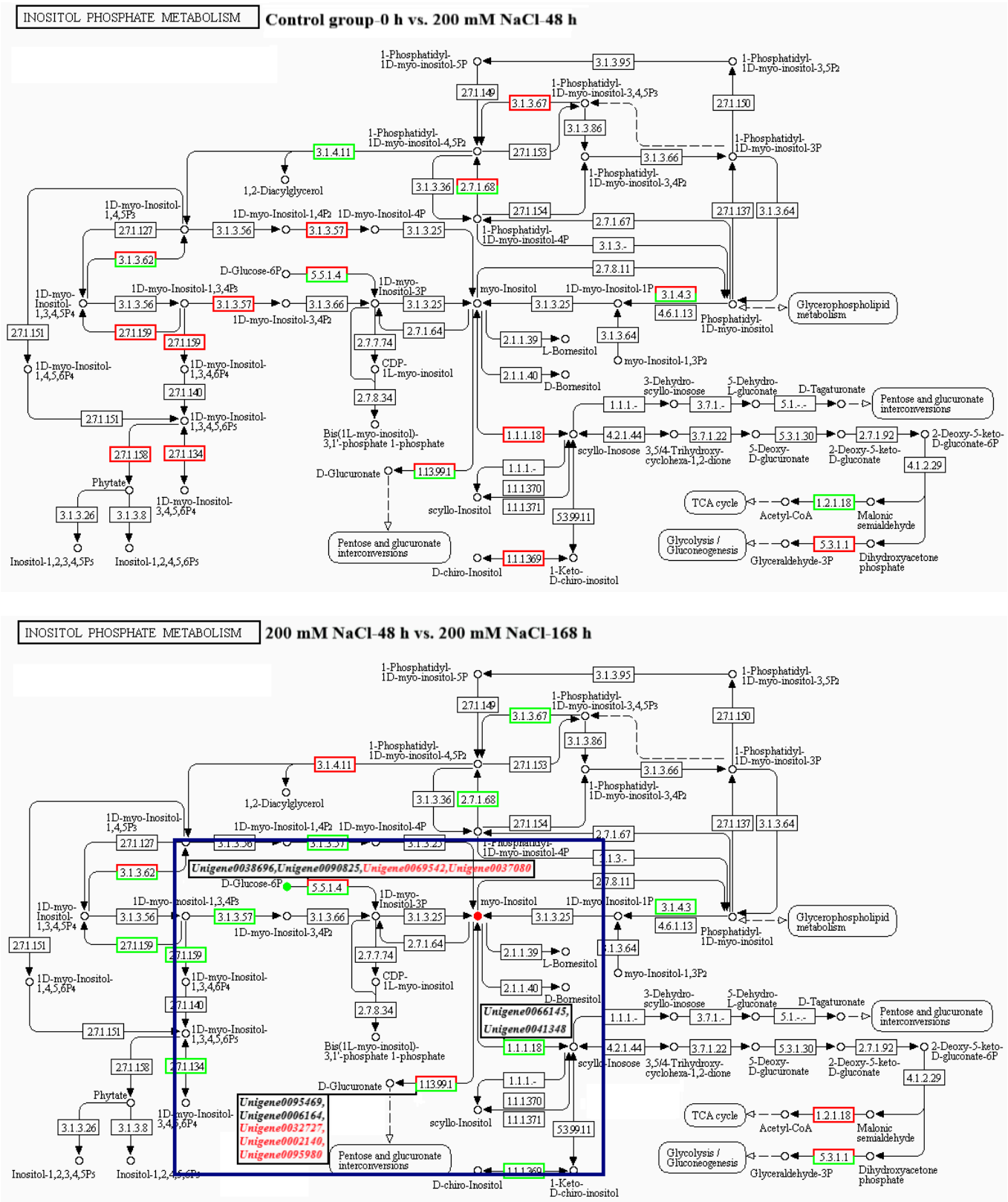

Figure 4. *Cont.*

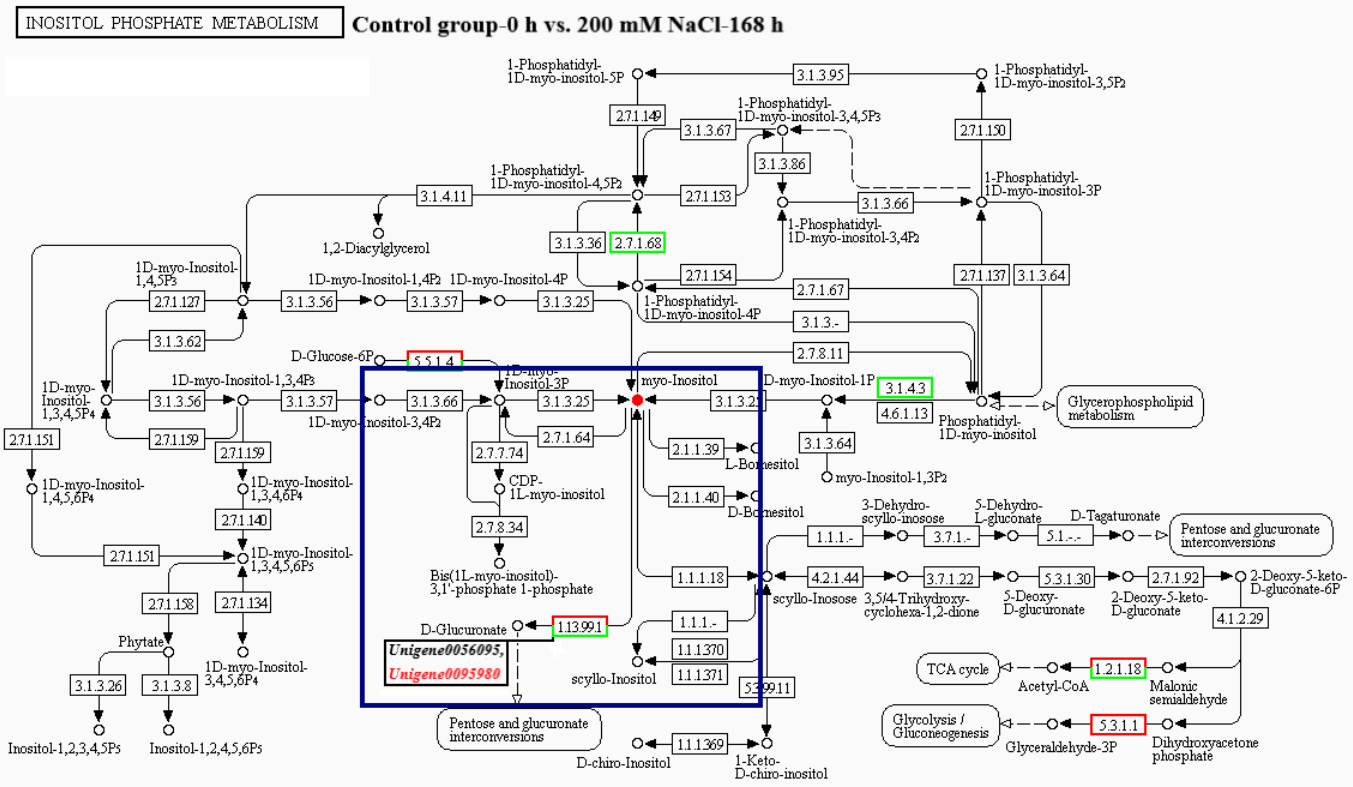

Figure 4. Analysis of the inositol phosphate metabolism pathway. (*T. ramosissima* root annotated DEGs and differential metabolites in the inositol phosphate metabolism pathway under NaCl stress at 0 h, 48 h, and 168 h. Note: blue box: DEGs annotated to metabolic pathways regulate the metabolism of different metabolites; ●: accumulation of differential metabolites; ●: degradation of differential metabolites; black genes in the box: down-regulation of differentially expressed gene expression levels; red genes in the box: up-regulation of differentially expressed gene expression levels).

3.5.3. Pearson Correlation Analysis of Differentially Expressed Genes and Their Related Differential Metabolites in the Inositol Phosphate Metabolism Pathway

Using the criteria of an absolute Pearson correlation coefficient |Corr| greater than 0.8 and a *p*-value less than 0.05, we analyzed the DEGs in the Inositol phosphate metabolism pathway and associated differential metabolites (Figure 4). From Figure 5, we can know that in the comparison group of Na-48 h vs. N-168 h, four DEGs (*Unigene0038696*, *Unigene0090825*, *Unigene0069542*, and *Unigene0037080*) are located downstream of D-Glucose 6-phosphate, modulate its degradation. *Unigene0038696* and *Unigene0090825* positively regulate the degradation of D-Glucose 6-phosphate, with no significant correlation. *Unigene0069542* and *Unigene0037080* negatively regulate the degradation of D-Glucose 6-phosphate, and *Unigene0037080* has a significant correlation with D-Glucose 6-phosphate. In the comparison group of 200 mM NaCl-48 h vs. 200 mM NaCl-168 h, five DEGs (*Unigene0095469*, *Unigene0006164*, *Unigene0032727*, *Unigene0002140*, and *Unigene0095980*) are located downstream of *Myo*-inositol, regulating its accumulation. Two DEGs (*Unigene0066145* and *Unigene0041348*), both up and downstream, regulate the accumulation of *Myo*-inositol. Among them, *Unigene0066145*, *Unigene0041348*, *Unigene0095469*, and *Unigene0006164* negatively regulate the accumulation of *Myo*-inositol, with no significant correlation. *Unigene0032727*, *Unigene0002140*, *and Unigene0095980* positively regulate the accumulation of *Myo*-inositol. In particular, *Unigene0002140 and Unigene0095980* positively regulate the accumulation of *Myo*-inositol, and they have a significant correlation. In the CK-0 h vs. N-168 h comparison group, two DEGs (*Unigene0056095* and *Unigene0095980*) are located downstream of *Myo*-inositol, regulating its accumulation. Among them, *Unigene0056095*

negatively regulates the accumulation of *Myo*-inositol. Notably, *Unigene0095980* positively regulates the accumulation of *Myo*-inositol and has a significant correlation.

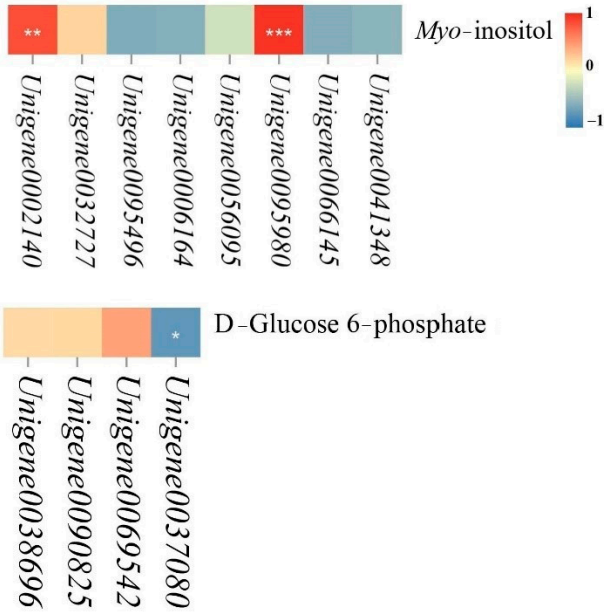

Figure 5. Pearson correlation analysis of DEGs and their related differential metabolites in the inositol phosphate metabolism pathway. (*T. ramosissima* roots under NaCl stress at 48 h and 168 h annotated DEGs and their related differential metabolites in the inositol phosphate metabolism pathway Pearson correlation analysis. Note: $p \geq 0.05$ is not marked; $0.01 < p < 0.05$ is marked as *; $0.001 < p < 0.01$ is marked as **; $p \leq 0.001$ is marked as ***).

3.6. Quantitative Real-Time PCR Validation of Candidate Genes in the Ascorbate and Aldarate Metabolism Pathway

In this study, we randomly selected 10 candidate genes for qRT-PCR to validate the reliability of the transcriptome sequencing data obtained. The findings indicate that the trends in gene expression from the qRT-PCR validation align with those from the transcriptome sequencing analysis (Supplementary Figure S6). This confirms the accuracy and reliability of the transcriptome data obtained in this study. It can, therefore, offer a scientific theoretical foundation and gene resources for identifying candidate genes in *T. ramosissima* roots that enhance salt tolerance and mitigate damage from NaCl stress.

4. Discussion

NaCl stress adversely affects plants by inducing osmotic stress, ion toxicity, nutritional imbalance, and oxidative stress, which can retard plant growth and even cause death [45–47]. In addition, excessive accumulation of ROS is a secondary stress that further impairs plant performance [48]. It causes oxidative damage to plants, affecting their growth and development [49]. When plants are subjected to NaCl stress, the integrity of the plant cell membrane is disrupted, ions become imbalanced, and ultimately ROS is produced. Excessive accumulation of ROS can cause oxidative stress, leading to cell death [50]. As the plants of the *Tamarix* genus have evolved under adverse conditions for a long time, they have developed a strong ability to self-regulate [33]. In our research, we delved into the relationship between differentially expressed genes (DEGs) and associated differential metabolites in the ascorbate and aldarate metabolism pathway in *T. ramosissima* roots subjected to 48 and 168 h of NaCl stress. This analysis provides valuable insights into enhancing plant salt tolerance and unravels the intricate physiological and molecular underpinnings of *T. ramosissima*'s salt tolerance.

Myo-inositol Oxygenase is an essential monooxygenase that can catalyze the transformation of *Myo*-inositol into D-Glucuronic acid (D-GlcUA) [51]. *Myo*-inositol Oxygenase plays a critical role in balancing the concentration of *Myo*-inositol, thereby aiding in the normal growth and development of plants [52]. In plants, *Myo*-inositol Oxygenase catalyzes the formation of D-GlcUA from *Myo*-inositol and activates D-GlcUA into UDP-GlcUA [53]. *Myo*-inositol Oxygenase and D-GlcUA in plant cells synthesize ascorbic acid, a crucial free radical scavenger, and antioxidant [54,55]. In rice (*Oryza sativa* L.), *OsMIOX* is expressed in the root system, and it can enhance plant tolerance under abiotic stress by reducing oxidative damage [56]. In other research, *Malus hupehensis*'s *MhMIOX2* has been shown to enhance the salt tolerance of poplar and *Arabidopsis* through heterologous expression [57]. Likewise, the heterologous expression of *MsMIOX2* in the yeast of *Medicago sativa* has improved the resistance to salt, salinity, drought, and cold [58]. In this study, we identified ten genes related to *Myo*-inositol oxygenase. Specifically, three genes (*Unigene0002140*, *Unigene0032727*, *Unigene0056095*) exhibited reduced expression at 48 h, followed by an increase at 168 h during NaCl stress. Five genes (*Unigene0006163*, *Unigene0006164*, *Unigene0006165*, *Unigene0032727*, and *Unigene0067118*) increased in expression level at 48 h under NaCl stress, and these genes significantly upregulated compared to the control group. Notably, *Unigene0095980* showed no change in expression level at 0 h and 48 h under NaCl stress. However, its expression level significantly increased at 168 h under NaCl stress. The results suggest that *Myo*-inositol oxygenase-related genes are consistently active at 48 h and 168 h under NaCl stress, enhancing plant tolerance against NaCl stress.

In the face of plant adversities, *Myo*-inositol and its derivatives play a crucial role in enhancing plant tolerance [59]. *Myo*-inositol serves as an osmoregulatory substance and ROS scavenger to protect plants from osmotic stress and oxidative damage, and as a signaling molecule, it regulates many metabolic pathways within plants, enhancing their salt tolerance [31]. Existing studies have shown that the expression of *Myo*-inositol transporter MfINT-like in alfalfa is induced by NaCl stress, and the ectopic expression of MfINT-like in transgenic tobacco enhances its tolerance to NaCl stress [60]. In quinoa (*Chenopodium quinoa* L.), the application of exogenous *Myo*-inositol under NaCl stress increases the activity of antioxidant enzymes, as well as the content of ascorbic acid and glutathione, improving quinoa's membrane stability, reducing oxidative damage, alleviating NaCl injury, and enhancing its salt tolerance [25]. Importantly, the halophyte ice plant (*Mesembryanthemum crystallinum*) can alleviate the dehydration effect of salt-stressed ice plant seedlings by decreasing the root Na^+/K^+ ratio and increasing the above-ground Na^+/K^+ ratio under the supply of *Myo*-inositol [61]. In this study, the content of *Myo*-inositol decreased initially and then increased after 48 h and 168 h of NaCl stress. Among the DEGs in the Na-48 h vs. N-168 h comparison group, six genes (*Unigene0095469*, *Unigene0006164*, *Unigene0032727*, *Unigene0056095*, *Unigene0002140*, and *Unigene0095980*) were found to be involved in the Ascorbate and aldarate metabolism pathway and Inositol phosphate metabolism pathway, regulating the accumulation of *Myo*-inositol downstream. Specifically, *Unigene0002140* and *Unigene0095980* positively regulated the accumulation of *Myo*-inositol and showed a significant correlation. In the CK-0 h vs. N-168 h comparison group, two DEGs (*Unigene0056095* and *Unigene0095980*) were found to be involved in the same metabolic pathways and regulated the accumulation of *Myo*-inositol. *Unigene0056095* negatively regulated *Myo*-inositol accumulation, while *Unigene0095980* positively regulated it with significant correlation. Therefore, *Unigene0002140* and *Unigene0095980*, as genes related to *Myo*-inositol oxygenase, play an important role in regulating *Myo*-inositol. The results indicate that *Myo*-inositol, as a precursor for the synthesis of ascorbic acid, indirectly promotes the antioxidant defense mechanism in plants. It acts as a compatible solute to maintain cell turgor and prevent cell dehydration under high salt conditions. Overall, *Myo*-inositol, along with genes associated with *Myo*-inositol oxygenase, actively engages in both the ascorbate and aldarate metabolism pathway and the inositol phosphate metabolism pathway. This engagement responds to NaCl stress by clearing excessive ROS accumulation, preserving cellular homeostasis, and enhancing the salt tolerance of

T. ramosissima. L-gulono-1,4-lactone serves as a direct precursor of ascorbic acid in plant cells, and it is a substrate of L-gulono-1,4-lactone oxidoreductase, which catalyzes the final step of ascorbic acid biosynthesis [62–64]. Ascorbic acid plays essential metabolic and antioxidative roles in living organisms [65–67]. In tobacco, wild-type (wt) plants had elevated ascorbic acid levels when fed L-gulono-1,4-lactone [68]. In tomato seedlings, exogenous ascorbic acid increased resistance to NaCl stress and reduced lipid peroxidation, promoting the survival rate of tomato seedlings [69]. In this study, in the Na-48 h vs. N-168 h comparison group, *Unigene0064911* was upstream of L-Gulono-1,4-lactone and positively regulated the accumulation of L-Gulono-1,4-lactone, showing a significant correlation. *Unigene0007112, Unigene0007113, Unigene0068803*, and *Unigene0105480* were downstream of L-Gulono-1,4-lactone and regulated its accumulation. In addition, *Unigene0007112* and *Unigene0007113* negatively regulated the accumulation of L-Gulono-1,4-lactone, with *Unigene0007112* showing a significant correlation with L-Gulono-1,4-lactone. *Unigene0068803* and *Unigene0105480* positively regulated the accumulation of L-Gulono-1,4-lactone. In the CK-0 h vs. N-168 h comparison group, *Unigene0105480* was downstream of L-Gulono-1,4-lactone and regulated its accumulation. Moreover, the content of L-Gulono-1,4-lactone in the roots of *T. ramosissima* decreased first and then increased under NaCl stress at 48 h and 168 h, suggesting that L-Gulono-1,4-lactone was involved in increasing ascorbic acid content and alleviating NaCl toxicity. Importantly, although *Unigene0105480* actively participated in regulating the accumulation of L-Gulono-1,4-lactone, its correlation with L-Gulono-1,4-lactone was not significant and required further validation. Additionally, other research has shown that under 200 mM NaCl stress, the ascorbate and aldarate metabolism pathway plays an important role in promoting and protecting the growth of cotton [70]. In this study, the roots of *T. ramosissima* under NaCl stress at 48 h and 168 h had 43 DEGs and four differentially regulated metabolites in the ascorbate and aldarate metabolism pathway responding to NaCl stress and mitigating the detrimental effects of NaCl stress on the growth of *T. ramosissima*.

5. Conclusions

Myo-inositol is pivotal to the growth and development of plants. Serving as an osmotic regulator and a ROS scavenger, inositol safeguards plants against osmotic stress and oxidative harm, bolstering their resilience to stress. In our research, after exposing *T. ramosissima* roots to 48 h and 168 h of NaCl stress, numerous genes associated with *Myo*-inositol oxygenase were identified to be involved in the ascorbate and aldarate metabolism pathway, as well as the inositol phosphate metabolism pathway. These genes effectively modulated the rise of metabolites like L-Gulono-1,4-lactone and *Myo*-inositol. Such metabolites are instrumental in fostering the growth, development, and defense mechanisms of *T. ramosissima* against NaCl stress, ensuring its regular progression. Specifically, these metabolites positively influence the accumulation of *Myo*-inositol within the aforementioned metabolic pathways and are closely correlated with *Myo*-inositol. Among these, *Unigene0002140* and *Unigene0095980* stand out as potential key genes associated with *Myo*-inositol, meriting further investigation.

Supplementary Materials: The following supporting information can be downloaded at: https://www.mdpi.com/article/10.3390/f14081686/s1, Supplementary Table S1: Sequences of specific primers. Supplementary Table S2: Pfam A protein domain analysis of *Myo*-inositol oxygenase-related genes. Supplementary Table S3: Log_2 fold-change of DEGs in the ascorbate and aldarate metabolism pathway. Supplementary Table S4: Analysis of differentially expressed metabolites in the ascorbate and aldarate metabolism pathway. Supplementary Table S5: Log_2 fold-change of DEGs in the inositol phosphate metabolism pathway. Supplementary Table S6: Analysis of differentially expressed metabolites in the inositol phosphate metabolism pathway. Supplementary Figure S1: Expression levels of *Myo*-inositol oxygenase-related genes. Supplementary Figure S2: Changes in expression levels of DEGs in the ascorbate and aldarate metabolism pathway. Supplementary Figure S3: Log_2 fold-change of differentially expressed metabolite content in the ascorbate and aldarate metabolism pathway. Supplementary Figure S4: Changes in expression levels of DEGs in the inos-

itol phosphate metabolism pathway. Supplementary Figure S5: Log_2 fold-change of differentially expressed metabolite content in the inositol phosphate metabolism pathway. Supplementary Figure S6: Validation of DEGs by qRT-PCR.

Author Contributions: Methodology, H.L. and Y.C.; Software, H.L., Y.F. and Y.C.; Formal analysis, H.L., Y.F. and Y.C.; Resources, Y.C.; Data curation, H.L., Y.F., H.Z. and Y.C.; Writing—original draft, H.L. and Y.C.; Writing—review & editing, H.L., Y.F., H.Z. and Y.C.; Project administration, H.L. and H.Z.; Funding acquisition, H.Z. All authors have read and agreed to the published version of the manuscript.

Funding: This work was jointly supported by grants from "Research on Key Techniques for Boosting Carbon Sequestration and Cultivating Energy Crops and Forests in Coastal Agroforestry Systems" (BE2022305).

Data Availability Statement: We uploaded our data to the NCBI database with an SRP number of SRP356215.

Conflicts of Interest: The authors declare no conflict of interest.

References

1. Singh, A. Soil salinization management for sustainable development: A review. *J. Environ. Manag.* **2021**, *277*, 111383. [CrossRef]
2. Uri, N. Cropland Soil Salinization and Associated Hydrology: Trends, Processes and Examples. *Water* **2018**, *10*, 1030. [CrossRef]
3. Muhetaer, N.; Nurmemet, I.; Abulaiti, A.; Xiao, S.; Zhao, J. A Quantifying Approach to Soil Salinity Based on a Radar Feature Space Model Using ALOS PALSAR-2 Data. *Remote Sens.* **2022**, *14*, 363. [CrossRef]
4. Rahman, M.M.; Mostofa, M.G.; Keya, S.S.; Siddiqui, M.N.; Ansary, M.M.U.; Das, A.K.; Rahman, M.A.; Tran, L.S. Adaptive mechanisms of halophytes and their potential in improving salinity tolerance in plants. *Int. J. Mol. Sci.* **2021**, *22*, 10733. [CrossRef] [PubMed]
5. Munns, R. Genes and salt tolerance: Bringing them together. *New Phytol.* **2005**, *167*, 645–663. [CrossRef] [PubMed]
6. Negrão, S.; Schmöckel, S.M.; Tester, M. Evaluating physiological responses of plants to salinity stress. *Ann. Bot.* **2017**, *119*, 1–11. [CrossRef]
7. Behera, T.K.; Krishna, R.; Ansari, W.A.; Aamir, M.; Kumar, P.; Kashyap, S.P.; Pandey, S.; Kole, C. Approaches involved in the vegetable crops Salt stress tolerance improvement: Present status and way ahead. *Front. Plant Sci.* **2021**, *12*, 787292. [CrossRef]
8. Lee, S.; Jeon, D.; Choi, S.; Kang, Y.; Seo, S.; Kwon, S.; Lyu, J.; Ahn, J.; Seo, J.; Kim, C. Expression profile of sorghum genes and Cis-regulatory elements under salt-stress conditions. *Plants* **2022**, *11*, 869. [CrossRef] [PubMed]
9. Shahid, M.A.; Sarkhosh, A.; Khan, N.; Balal, R.M.; Ali, S.; Rossi, L.; Gómez, C.; Mattson, N.; Nasim, W.; Garcia-Sanchez, F. Insights into the physiological and biochemical impacts of salt stress on plant growth and development. *Agronomy* **2020**, *10*, 938. [CrossRef]
10. Ma, L.; Liu, X.; Lv, W.; Yang, Y. Molecular mechanisms of plant responses to salt stress. *Front. Plant Sci.* **2022**, *13*, 934877. [CrossRef]
11. Hasegawa, P.M.; Bressan, R.A.; Zhu, J.K.; Bohnert, H.J. Plant cellular and molecular response to high salinity. *Annu. Rev. Plant Physiol. Plant Mol. Biol.* **2000**, *51*, 463–499. [CrossRef] [PubMed]
12. Akram, N.A.; Shafiq, F.; Ashraf, M. Ascorbic acid-a potential oxidant scavenger and its role in plant development and abiotic stress tolerance. *Front. Plant Sci.* **2017**, *8*, 613. [CrossRef] [PubMed]
13. Chartzoulakis, K.; Psarras, G. Global change effects on crop photosynthesis and production in mediterranean: The case of crete, greece. *Agric. Ecosyst. Environ.* **2005**, *106*, 147–157. [CrossRef]
14. Sun, J.K.; Li, T.; Xia, J.B.; Tian, J.Y.; Lu, Z.H.; Wang, R.T. Influence of salt stress on ecophysiological parameters of *Periploca sepium* bunge. *Plant Soil Environ.* **2011**, *57*, 139–144. [CrossRef]
15. Isayenkov, S.V.; Maathuis, F.J.M. Plant salinity stress: Many unanswered questions remain. *Front. Plant Sci.* **2019**, *10*, 80. [CrossRef]
16. Zhang, W.; Liu, S.; Li, C.; Zhang, P.; Zhang, P. Transcriptome sequencing of antarctic moss under salt stress emphasizes the important roles of the ROS-scavenging system. *Gene* **2019**, *696*, 122–134. [CrossRef]
17. Zheng, Y.; Jia, A.; Ning, T.; Xu, J.; Li, Z.; Jiang, G. Potassium nitrate application alleviates sodium chloride stress in winter wheat cultivars differing in salt tolerance. *J. Plant Physiol.* **2008**, *165*, 1455–1465. [CrossRef]
18. Noctor, G.; Reichheld, J.; Foyer, C.H. ROS-related redox regulation and signaling in plants. *Semin. Cell Dev. Biol.* **2018**, *80*, 3–12. [CrossRef]
19. Abbasi, H.; Jamil, M.; Haq, A.; Ali, S.; Ahmad, R.; Malik, Z. Parveen salt stress manifestation on plants, mechanism of salt tolerance and potassium role in alleviating it: A review. *Zemdirbyste* **2016**, *103*, 229–238. [CrossRef]
20. Ardie, S.W.; Xie, L.; Takahashi, R.; Liu, S.; Takano, T. Cloning of a high-affinity K^+ transporter gene *PutHKT2;1* from *Puccinellia tenuiflora* and its functional comparison with *OsHKT2;1* from rice in yeast and *Arabidopsis*. *J. Exp. Bot.* **2009**, *60*, 3491–3502. [CrossRef]

21. Loewus, M.W.; Sasaki, K.; Leavitt, A.L.; Munsell, L.; Sherman, W.R.; Loewus, F.A. Enantiomeric form of *Myo*-inositol-1-phosphate produced by *Myo*-inositol-1-phosphate synthase and *Myo*-inositol kinase in higher plants. *Plant Physiol.* **1982**, *70*, 1661–1663. [CrossRef]
22. Kılbaş, B.; Balci, M. Recent advances in inositol chemistry: Synthesis and applications. *Tetrahedron* **2011**, *67*, 2355–2389. [CrossRef]
23. Loewus, F.A.; Murthy, P.P.N. myo-Inositol metabolism in plants. *Plant Sci.* **2000**, *150*, 1–19. [CrossRef]
24. Valluru, R.; Van den Ende, W. *Myo*-inositol and beyond--emerging networks under stress. *Plant Sci.* **2011**, *181*, 387–400. [CrossRef]
25. Al-Mushhin, A.; Qari, S.; Fakhr, M.; Alnusairi, G.; Alnusaire, T.; ALrashidi, A.; Latef, A.; Ali, O.; Khan, A.; Soliman, M. Exogenous *Myo*-inositol alleviates salt stress by enhancing antioxidants and membrane stability via the upregulation of stress responsive genes in *Chenopodium quinoa* L. *Plants* **2021**, *10*, 2416. [CrossRef]
26. Jia, Q.; Kong, D.; Li, Q.; Sun, S.; Song, J.; Zhu, Y.; Liang, K.; Ke, Q.; Lin, W.; Huang, J. The function of inositol phosphatases in plant tolerance to abiotic stress. *Int. J. Mol. Sci.* **2019**, *20*, 3999. [CrossRef]
27. Michell, R.H. Inositol derivatives: Evolution and functions. *Nat. Rev. Mol. Cell Bio.* **2008**, *9*, 151–161. [CrossRef] [PubMed]
28. Kindl, H.; Hoffmann-ostenhof, O. Studies on the biosynthsis of cyclitols.II. formation of meso-inositol from C14-1-Glucose in *Sinapis alba* and selective degradation of the resulting product. *Biochem Z* **1964**, *339*, 374–381. [PubMed]
29. Majumder, A.L.; Johnson, M.D.; Henry, S.A. 1L-myo-inositol-1-phosphate synthase. *Biochim. Biophys. Acta* **1997**, *1348*, 245–256. [CrossRef]
30. Kusuda, H.; Koga, W.; Kusano, M.; Oikawa, A.; Saito, K.; Hirai, M.Y.; Yoshida, K.T. Ectopic expression of *Myo*-inositol 3-phosphate synthase induces a wide range of metabolic changes and confers salt tolerance in rice. *Plant Sci.* **2015**, *232*, 49–56. [CrossRef]
31. Klages, K.; Boldingh, H.; Smith, G.S. Accumulation of *Myo*-inositol in actinidia seedlings subjected to Salt Stress. *Ann. Bot.* **1999**, *84*, 521–527. [CrossRef]
32. Hu, L.; Zhou, K.; Li, Y.; Chen, X.; Liu, B.; Li, C.; Gong, X.; Ma, F. Exogenous *Myo*-inositol alleviates salinity-induced stress in *Malus hupehensis* Rehd. *Plant Physiol. Biochem.* **2018**, *133*, 116–126. [CrossRef] [PubMed]
33. Wang, Z.; He, Z.; Xu, X.; Shi, X.; Ji, X.; Wang, Y. Revealing the salt tolerance mechanism of *Tamarix hispida* by large-scale identification of genes conferring salt tolerance. *Tree Physiol.* **2021**, *41*, 2153–2170. [CrossRef] [PubMed]
34. Thomson, W.W.; Liu, L.L. Ultrastructural features of the salt gland of *Tamarix aphylla* L. *Planta* **1967**, *73*, 201–220. [CrossRef]
35. Wei, X.; Yan, X.; Yang, Z.; Han, G.; Wang, L.; Yuan, F.; Wang, B. Salt glands of recretohalophyte *Tamarix* under salinity: Their evolution and adaptation. *Ecol. Evol.* **2020**, *10*, 9384–9395. [CrossRef]
36. Lu, Y.; Lei, J.Q.; Zeng, F.J.; Xu, L.S.; Peng, S.L.; Gao, H.H.; Liu, G.J. Effects of NaCl treatment on growth and Ec-ophysiology Characteristics of *Tamarix ramossisma*. *J. Des. Res.* **2014**, *34*, 1509–1515. (In Chinese) [CrossRef]
37. Wang, J.; Zou, A.; Xiang, S.; Liu, C.; Peng, H.; Wen, Y.; Ma, X.; Chen, H.; Ran, M.; Sun, X. Transcriptome analysis reveals the mechanism of zinc ion-mediated plant resistance to TMV in Nicotiana benthamiana. *Pestic. Biochem. Phys.* **2022**, *184*, 105100. [CrossRef]
38. Chen, Y.; Wang, G.; Zhang, H.; Zhang, N.; Jiang, J.; Song, Z. Transcriptome analysis of *Tamarix ramosissima* leaves in response to NaCl stress. *PLoS ONE* **2022**, *17*, e265653. [CrossRef]
39. Conesa, A.; Gotz, S.; Garcia-Gomez, J.M.; Terol, J.; Talon, M.; Robles, M. Blast2GO: A universal tool for annotation, visualization and analysis in functional genomics research. *Bioinformatics* **2005**, *21*, 3674–3676. [CrossRef]
40. Ashburner, M.; Ball, C.A.; Blake, J.A.; Botstein, D.; Butler, H.; Cherry, J.M.; Davis, A.P.; Dolinski, K.; Dwight, S.S.; Eppig, J.T.; et al. Gene Ontology: Tool for the unification of biology. *Nat. Genet.* **2000**, *25*, 25–29. [CrossRef]
41. Chen, Y.; Zhang, S.; Du, S.; Zhang, X.; Jiang, J.; Wang, G. Analysis of amino acids in the roots of *Tamarix ramosissima* by application of exogenous potassium (K^+) under NaCl Stress. *Int. J. Mol. Sci.* **2022**, *23*, 9331. [CrossRef] [PubMed]
42. Chen, Y.; Zhang, S.; Du, S.; Jiang, J.; Wang, G. Transcriptome and metabonomic analysis of *Tamarix ramosissima* potassium (K^+) channels and transporters in response to NaCl Stress. *Genes* **2022**, *13*, 1313. [CrossRef] [PubMed]
43. Livak, K.J.; Schmittgen, T.D. Analysis of relative gene expression data using real-time quantitative PCR and the $2^{-\Delta\Delta CT}$ Method. *Methods* **2001**, *25*, 402–408. [CrossRef]
44. Finn, R.D.; Coggill, P.; Eberhardt, R.Y.; Eddy, S.R.; Mistry, J.; Mitchell, A.L.; Potter, S.C.; Punta, M.; Qureshi, M.; Sangrador-Vegas, A.; et al. The Pfam protein families database: Towards a more sustainable future. *Nucleic Acids Res.* **2016**, *44*, D279–D285. [CrossRef] [PubMed]
45. Zhu, J. Salt and drought stress signal transduction in plants. *Annu. Rev. Plant Biol.* **2002**, *53*, 247–273. [CrossRef] [PubMed]
46. Zhao, S.; Zhang, Q.; Liu, M.; Zhou, H.; Ma, C.; Wang, P. Regulation of plant responses to salt stress. *Int. J. Mol. Sci.* **2021**, *22*, 4609. [CrossRef]
47. Cimini, S.; Locato, V.; Giacinti, V.; Molinari, M.; De Gara, L. A Multifactorial regulation of glutathione metabolism behind salt tolerance in rice. *Antioxidants* **2022**, *11*, 1114. [CrossRef]
48. Liu, J.; Fu, C.; Li, G.; Khan, M.N.; Wu, H. ROS Homeostasis and plant salt tolerance: Plant nanobiotechnology updates. *Sustainability* **2021**, *13*, 3552. [CrossRef]
49. Hasanuzzaman, M.; Raihan, M.; Masud, A.; Rahman, K.; Nowroz, F.; Rahman, M.; Nahar, K.; Fujita, M. Regulation of reactive oxygen species and antioxidant defense in plants under salinity. *Int. J. Mol. Sci.* **2021**, *22*, 9326. [CrossRef]
50. Ahmad, P.; Jaleel, C.A.; Salem, M.A.; Nabi, G.; Sharma, S. Roles of enzymatic and nonenzymatic antioxidants in plants during abiotic stress. *Crit. Rev. Biotechnol.* **2010**, *30*, 161–175. [CrossRef]

51. Munir, S.; Mumtaz, M.A.; Ahiakpa, J.K.; Liu, G.; Chen, W.; Zhou, G.; Zheng, W.; Ye, Z.; Zhang, Y. Genome-wide analysis of *Myo*-inositol oxygenase gene family in tomato reveals their involvement in ascorbic acid accumulation. *BMC Genom.* **2020**, *21*, 284. [CrossRef] [PubMed]
52. Loewus, F.A.; Loewus, M.W. *Myo*-inositol: Its biosynthesis and metabolism. *Annu. Rev. Plant Physiol.* **1983**, *34*, 137–161. [CrossRef]
53. Kanter, U.; Usadel, B.; Guerineau, F.; Li, Y.; Pauly, M.; Tenhaken, R. The inositol oxygenase gene family of *arabidopsis* is involved in the biosynthesis of nucleotide sugar precursors for cell-wall matrix polysaccharides. *Planta* **2005**, *221*, 243–254. [CrossRef]
54. Shao, H.; Chu, L.; Shao, M.; Jaleel, C.A.; Hong-mei, M. Higher plant antioxidants and redox signaling under environmental stresses. *Comptes Rendus Biol.* **2008**, *331*, 433–441. [CrossRef]
55. Chen, X.; Zhou, Y.; Cong, Y.; Zhu, P.; Xing, J.; Cui, J.; Xu, W.; Shi, Q.; Diao, M.; Liu, H.Y. Ascorbic acid-induced photosynthetic adaptability of processing tomatoes to salt stress probed by fast OJIP fluorescence rise. *Front. Plant Sci.* **2021**, *12*, 594400. [CrossRef]
56. Duan, J.; Zhang, M.; Zhang, H.; Xiong, H.; Liu, P.; Ali, J.; Li, J.; Li, Z. *OsMIOX*, a *Myo*-inositol oxygenase gene, improves drought tolerance through scavenging of reactive oxygen species in rice (*Oryza sativa* L.). *Plant Sci.* **2012**, *196*, 143–151. [CrossRef] [PubMed]
57. Yang, J.; Yang, J.; Zhao, L.; Gu, L.; Wu, F.; Tian, W.; Sun, Y.; Zhang, S.; Su, H.; Wang, L. Ectopic expression of a *Malus hupehensis* Rehd. *Myo- inositol oxygenase gene (MhMIOX2) enhances tolerance to salt stress. Sci. Hortic.* **2021**, *281*, 109898. [CrossRef]
58. Guo, W.; Yu, D.; Zhang, R.; Zhao, W.; Zhang, L.; Wang, D.; Sun, Y.; Guo, C. Genome-wide identification of the *Myo*-inositol oxygenase gene family in alfalfa (*Medicago sativa* L.) and expression analysis under abiotic stress. *Plant Physiol. Biochem.* **2023**, *200*, 107787. [CrossRef]
59. Hu, L.; Zhou, K.; Liu, Y.; Yang, S.; Zhang, J.; Gong, X.; Ma, F. Overexpression of *MdMIPS1* enhances salt tolerance by improving osmosis, ion balance, and antioxidant activity in transgenic apple. *Plant Sci.* **2020**, *301*, 110654. [CrossRef]
60. Sambe, M.A.; He, X.; Tu, Q.; Guo, Z. A cold-induced *Myo*-inositol transporter-like gene confers tolerance to multiple abiotic stresses in transgenic tobacco plants. *Physiol. Plant* **2015**, *153*, 355–364. [CrossRef]
61. Li, C.H.; Tien, H.J.; Wen, M.F.; Yen, H.E. Myo-inositol transport and metabolism participate in salt tolerance of halophyte ice plant seedlings. *Physiol. Plant* **2021**, *172*, 1619–1629. [CrossRef]
62. Wheeler, G.L.; Jones, M.A.; Smirnoff, N. The biosynthetic pathway of vitamin C in higher plants. *Nature* **1998**, *393*, 365–369. [CrossRef]
63. Wolucka, B.A.; Communi, D. Mycobacterium tuberculosis possesses a functional enzyme for the synthesis of vitamin C, L-gulono-1,4-lactone dehydrogenase. *FEBS J.* **2006**, *273*, 4435–4445. [CrossRef] [PubMed]
64. Wolucka, B.A.; Van Montagu, M. GDP-Mannose 3′,5′-Epimerase Forms GDP-L-gulose, a putative intermediate for the de novo biosynthesis of Vitamin C in Plants. *J. Biol. Chem.* **2003**, *278*, 47483–47490. [CrossRef] [PubMed]
65. Smirnoff, N. Ascorbic acid metabolism and functions: A comparison of plants and mammals. *Free Radic. Biol. Med.* **2018**, *122*, 116–129. [CrossRef] [PubMed]
66. Qian, H.F.; Peng, X.F.; Han, X.; Ren, J.; Zhan, K.Y.; Zhu, M. stress factor, exogenous ascorbic acid, affects plant growth and the antioxidant system in *Arabidopsis thaliana*. *Russ. J. Plant Physl.* **2014**, *61*, 467–475. [CrossRef]
67. Foyer, C.H.; Noctor, G. Ascorbate and glutathione: The heart of the redox hub. *Plant Physiol.* **2011**, *155*, 2–18. [CrossRef]
68. Radzio, J.A.; Lorence, A.; Chevone, B.I.; Nessler, C.L. L-Gulono-1,4-lactone oxidase expression rescues vitamin C-deficient *Arabidopsis* (vtc) mutants. *Plant Mol. Biol.* **2003**, *53*, 837–844. [CrossRef]
69. Shalata, A.; Neumann, P.M. Exogenous ascorbic acid (vitamin C) increases resistance to salt stress and reduces lipid peroxidation. *J. Exp. Bot.* **2001**, *52*, 2207–2211. [CrossRef]
70. Akbar, A.; Han, B.; Khan, A.H.; Feng, C.; Ullah, A.; Khan, A.S.; He, L.; Yang, X. A transcriptomic study reveals salt stress alleviation in cotton plants upon salt tolerant PGPR inoculation. *Environ. Exp. Bot.* **2022**, *200*, 104928. [CrossRef]